

Electronic Supplementary Information (ESI)

Copper sulfide nanoparticles coated with Fe-EGCG networks for targeted MR imaging and chemo/photothermal/chemodynamic synergetic therapy of tumors

Na Liu,^a Risong Pan,^b Shuoshuo Su,^a Tianshu Yao,^b Yu Fan,^c and Jingyi Zhu^{*a}

^a School of Pharmaceutical Sciences, Nanjing Tech University, Nanjing 211816, People's Republic of China

^b College of Biotechnology and Pharmaceutical Engineering, Nanjing Tech University, Nanjing 211816, People's Republic of China

^c Department of Polymeric Materials, School of Materials Science and Engineering, Tongji University, Shanghai 201804, People's Republic of China

* To whom correspondence should be addressed. Tel: +86 25 5813 9942; fax: +86 25 58139942.

E-mail address: zhuji1210@njtech.edu.cn (J. Zhu)

Experimental section

Materials

Bifunctional polyethylene glycol terminated with amino and carboxyl groups (NH₂-PEG-COOH, Mw = 2000) and polyethylene glycol monomethyl ether terminated with carboxyl group (*m*PEG-COOH, Mw = 2000) were obtained from Shanghai Yayi Biotechnology Corporation (Shanghai, China). Folic acid (FA), cupric chloride dihydrate (CuCl₂·2H₂O), sodium sulfide nonahydrate (Na₂S·9H₂O), (-)-epigallocatechin gallate (EGCG), and glutathione (GSH) were purchased from Shanghai Macklin Biochemical Technology Co., Ltd. (Shanghai, China). Hyperbranched polyethylenimine (PEI.NH₂, Mw = 25000), 1-ethyl-3-(3-(dimethylamino)propyl) carbodiimide hydrochloride (EDC), and N-hydroxy succinimide (NHS) were provided from Sigma-Aldrich (St. Louis, MO). Dimethyl sulfoxide (DMSO) was purchased from Shanghai Aladdin Biochemical Technology Co., Ltd. (Shanghai, China). Fluorescein isothiocyanate (FI), phosphate buffered saline (PBS), normal saline (NS), and regenerated cellulose dialysis membranes with the molecular weight cut-off (MWCO) of 1000 and 8000-14000 were purchased from Shanghai Yuanye Biotechnology Co., Ltd. (Shanghai, China). Triethylamine and acetic anhydride were obtained from Sinopharm Chemical Reagent Co., Ltd. (Shanghai, China). Hydrogen peroxide (H₂O₂) was purchased from Shanghai Lingfeng Chemical Reagent Co., Ltd (Shanghai, China). Iron (III) chloride (FeCl₃) and methylene blue (MB) were obtained from Shanghai Titan Technology Co., Ltd (Shanghai, China). Dulbecco's modified eagle medium (DMEM), minimum essential medium (MEM), and fetal bovine serum (FBS) were purchased from Gibco (Carlsbad, CA). Penicillin and streptomycin were obtained from Gino Biomedical Technology Co., Ltd. (Hangzhou, China). Cell counting kit-8 (CCK-8) was purchased from 7Sea Biotech Co., Ltd. (Shanghai, China). Annexin V-labeled fluorescein isothiocyanate (FITC)/propidium

iodide (PI) apoptosis detection kit, 2',7'-dichlorofluorescein diacetate (DCFH-DA) reactive oxygen species assay kit, and GSH/oxidized GSH (GSSG) colorimetric assay kit were provided by Beyotime Biotechnology (Shanghai, China). Lipid peroxidation assay kit with probe C11-BODIPY^{581/591} was purchased from GlpBio Technology (Montclair, CA). Water used in all experiments was purified using a Milli-Q Plus 185 water purification system (Millipore, Bedford, MA) with a resistivity higher than 18.2 M Ω ·cm.

Synthesis of FA-PEG-COOH

The carboxyl-terminated PEGylated FA (FA-PEG-COOH) was synthesized *via* the amide coupling reaction between FA and NH₂-PEG-COOH using carbodiimide catalytic chemistry, as described in the previous literature.¹ Firstly, FA (33.11 mg, 75.00 μ mol) dispersed in DMSO (10 mL) was activated by the DMSO solution containing equal molar equivalent of EDC (14.38 mg, 75.00 μ mol, 5 mL) and NHS (8.63 mg, 75.00 μ mol, 3 mL) through carbodiimide catalytic chemistry. After 3 h magnetic stirring, the activated carboxyl of FA was reacted with the amine group of NH₂-PEG-COOH (100.00 mg, 50.00 μ mol) dissolved in DMSO (15 mL) at the 1.5:1 molar ratio between FA and NH₂-PEG-COOH under stirring condition for 72 h. Ultimately, the above reaction mixture was dialyzed in water (9 times, 2 L) through a dialysis membrane with MWCO of 1000 for 3 days to remove the excess reactants or by-products, followed by lyophilization to obtain FA-PEG-COOH (yield = 86.77%).

Synthesis of PEI.NH₂-(PEG-FA)-FI

Subsequently, the multifunctional polyethylenimine nanosystem with FA-PEG-COOH linking and FI conjugating was constructed according to the protocol outlined in Scheme 1a. Briefly, FA-PEG-COOH (41.33 mg, 18.00 μ mol) dispersed in 10 mL water was activated by the aqueous mixture of EDC (34.51 mg, 180.00 μ mol, 10 mL) and NHS (20.72 mg, 180.00 μ mol, 5 mL) under constant

magnetic stirring at 25 °C for 3 h. Then, the activated FA-PEG-COOH (20 molar equivalents) aqueous solution was reacted with the aqueous solution of PEI.NH₂ (22.50 mg, 0.90 μmol, 10 mL) *via* the amide coupling reaction for 72 h to generate PEI.NH₂-(PEG-FA). The obtained reaction mixture was subjected to dialysis and lyophilization to acquire PEI.NH₂-(PEG-FA) powder (yield = 80.21%) referring to the similar purification procedure of FA-PEG-COOH, except using a 8000-14000 MWCO dialysis membrane. Finally, the FI conjugation reaction was conducted by dropwise adding 2 mL DMSO containing FI (1.95 mg, 5.00 μmol, 5 molar equivalents) to 13 mL DMSO solution of PEI.NH₂-(PEG-FA) (56.67 mg, 1.00 μmol) under constant stirring at 25 °C. After 24 h reaction in a light-avoiding environment, the multifunctional nanoplatform PEI.NH₂-(PEG-FA)-FI was obtained. The PEI.NH₂-(PEG-FA)-FI powder (yield = 78.30%) was collected utilizing the steps similar to the purification process of PEI.NH₂-(PEG-FA). Parallel control experiments were conducted to prepare FA-free nanosystem (PEI.NH₂-*m*PEG-FI, yield = 77.97%) under the identical reaction conditions, with the sole modification of *m*PEG-COOH substituted for FA-PEG-COOH.

Formation of FA-CuS PENs@Fe-EGCG nanocomposites

The pre-synthesized PEI.NH₂-(PEG-FA)-FI was then employed as a nano-template to construct copper sulfide nanoparticles (CuS NPs) coated with iron ion-EGCG (Fe-EGCG) metal polyphenolic networks (MPNs) according to the previous synthesis method published in the literature.²⁻⁴ Briefly, the aqueous solution of CuCl₂·2H₂O (6.39 mg, 37.50 μmol, 5 mL) was mixed with the aqueous solution of PEI.NH₂-(PEG-FA)-FI (43.22 mg, 0.75 μmol, 10 mL) under constant stirring in the dark for 15 min. Subsequently, the aqueous solution of Na₂S·9H₂O (27.02 mg, 112.50 μmol, 10 mL) was dropwise added into the resulting mixture at 70 °C with continuous stirring for 30 min, enabling the *in situ* formation of CuS NPs within the internal cavity of PEI.NH₂-(PEG-FA)-FI. After the above

solution cooled to 25 °C, triethylamine (79.34 μL , 564.20 μmol) and acetic anhydride (52.87 μL , 564.20 μmol) were successively added to the cooled solution to acetylate the residual primary amines of PEI.NH₂-(PEG-FA)-FI in a 5:1 molar ratio relative to surface amines *via* 24 h stirring. Finally, the FA-functionalized polyethylenimine entrapped CuS NPs (FA-CuS PENs, yield = 70.08%) were purified utilizing the same purification protocol as PEI.NH₂-(PEG-FA)-FI. Parallel control experiments were also performed to prepare FA-free CuS PENs (yield = 75.55%) utilizing PEI.NH₂-*m*PEG-FI as a nano-template under the identical reaction conditions.

The FeCl₃ aqueous solution (8 mM, 313.00 μL) was gradually introduced into the FA-CuS PENs aqueous solution (15.20 mg, 0.25 μmol , 5 mL) under continuous vortex mixing to ensure homogeneous dispersion. Subsequently, the EGCG aqueous solution (8 mM, 625.00 μL) was added dropwise with constant stirring, and the reaction mixture was maintained in the dark for 24 h to facilitate complete formation of MPNs. The molar ratio of FeCl₃ to EGCG was maintained at 1:2. Upon completion of the reaction, the resulting solution underwent ultrafiltration purification with a 3000 MWCO membrane to collect the FA-CuS PENs@Fe-EGCG supernatant. The purified supernatant was finally freeze-dried to yield FA-CuS PENs@Fe-EGCG nanocomposites (yield = 87.10%), while the filtrate was retained to quantify unloaded EGCG. Parallel control experiments were performed to prepare FA-free CuS PENs@Fe-EGCG nanocomposites (yield = 91.95%) and iron ion-free FA-CuS PENs@EGCG nanocomposites (yield = 78.75%) under the identical reaction conditions for subsequent comparative analysis.

Characterization techniques

Proton nuclear magnetic resonance (¹H NMR) spectra were recorded using a Bruker AV-400 NMR spectrometer. All samples were uniformly dispersed in 600 μL deuterium oxide (D₂O) before

measurements. Ultraviolet-Visible (UV-Vis) spectra were collected using a UV-1800PC UV-Vis spectrophotometer (MAPADA, Shanghai, China). Transmission electron microscopy (TEM) imaging was executed using a JEOL 2010F analytical electron microscope (JEOL, Tokyo, Japan) operating at 200 kV. The solutions of FA-CuS PENs@Fe-EGCG and FA-CuS PENs@EGCG nanocomposites pre-dissolved in water or phosphate buffer (1 mg/mL, 10 μ L) were separately dropped onto carbon-coated copper grids and air-dried before measurements. The size distribution histograms of the FA-CuS PENs@Fe-EGCG and FA-CuS PENs@EGCG nanocomposites were measured using ImageJ software after randomly selecting and analyzing more than 300 NPs from each sample's TEM images. X-ray photoelectron spectroscopy (XPS) measurements were performed using PHI 5000 Versa Probe X-ray photoelectron spectrometer (a monochromatic Al K Alpha X-ray radiation). Zeta potential and dynamic light scattering (DLS) measurements were conducted using a Malvern Zetasizer Nano ZS90 system (Worcestershire, UK) coupled with a standard laser with a wavelength of 633 nm. The Cu and Fe contents of the pre-synthesized nanocomposites were determined by a Leeman Prodigy inductively coupled plasma-optical emission spectroscopy (ICP-OES, Hudson, NH, USA) after complete digestion with aqua regia.

Determination of EGCG loading efficiency

The EGCG loading efficiency was determined by measuring the absorbance of the retained filtrate at 273 nm (the characteristic peak of EGCG) using UV-Vis spectroscopy upon purifying the FA-CuS PENs@Fe-EGCG, FA-CuS PENs@EGCG, and CuS PENs@Fe-EGCG nanocomposites solutions. The mass of free EGCG in the retained filtrate was determined based on the pre-established standard curve of EGCG aqueous solution with different concentrations. Subsequently, the mass of EGCG loaded into the nanocomposites was determined by deducting the mass of free EGCG from the total

mass of initial EGCG used in the synthesis. Finally, the drug loading amount (DL) and encapsulation efficiency (EE) of EGCG were calculated on the basis of the following formulas:

$$DL (\%) = (W_E/W_N) \times 100\%$$

$$EE (\%) = (W_E/W_0) \times 100\%$$

Where W_E represents the mass of loaded EGCG, W_N represents the mass of the corresponding nanocomposites, and W_0 represents the total mass of initial EGCG utilized in the nanocomposites synthesis.

Hemolysis assay

Hemolysis assay was performed to evaluate the hemocompatibility of the FA-CuS PENs@Fe-EGCG nanocomposites according to the literature.⁴ All animal experiments were conducted with the permission of the Animal Ethics Committee of Nanjing Tech University (No. IACUC-20250306-70) for animal care and use. Firstly, whole blood (1 mL) obtained through orbital blood extraction from healthy nude mice was added into a Eppendorf (EP) tube containing heparin sodium, followed by centrifuging (3000 rpm, 5 min), washing and discarding the supernatant to collect red blood cells. The prepared red blood cell pellet was resuspended in PBS and diluted 30 times. Afterwards, 500 μ L of the diluted red blood cell suspension was mixed separately with 500 μ L PBS (negative control), 500 μ L water (positive control), and 500 μ L PBS solution of FA-CuS PENs@Fe-EGCG nanocomposites with different Fe concentrations (5, 10, 25, 50, and 100 μ M). After 2 h incubation at 37°C, all the samples were subjected to centrifugation (10000 rpm, 5 min). Subsequently, the photograph of samples was taken and the absorbance of the obtained supernatant at 540 nm was measured *via* UV-Vis spectrometry. The hemolysis rate was calculated on the basis of the equation published in the literature.^{4, 5}

Photothermal performance of FA-CuS PENs@Fe-EGCG nanocomposites

The photothermal performance of FA-CuS PENs@Fe-EGCG nanocomposites was explored *via* 1064 nm near infrared (NIR) laser irradiation from the perspectives of concentration, laser power intensity, and thermal stability. Initially, the 500 μ L EP tubes containing 100 μ L of FA-CuS PENs@Fe-EGCG aqueous solutions with a series of Cu concentrations (0.15, 0.3, 0.6, and 1.2 mM) were exposed to continuous laser irradiation (1064 nm, 1.0 W/cm²) for 5 min. Meanwhile, an equal volume of water was employed as a control and subjected to laser irradiation under the identical conditions. The temperature change trend of each sample was monitored per 5 s utilizing the thermocouple probe (DT-8891E, Shenzhen Everbest Machinery Industry Co., Ltd., Shenzhen, China). Additionally, the temperature change trends of FA-CuS PENs@Fe-EGCG aqueous solution ([Cu] = 0.6 mM, 100 μ L) irradiated by a 1064 nm laser at gradually increased power intensities (0.6, 1.0, 1.5, and 2.0 W/cm²) were also detected by thermocouple probe to reflect the photothermal efficacy. Finally, the photothermal stability of FA-CuS PENs@Fe-EGCG aqueous solution ([Cu] = 0.6 mM, 100 μ L) was assessed by plotting the temperature profiles of laser irradiation (1064 nm, 1.0 W/cm²) mediated heating and natural cooling processes over time in five consecutive cycles. Afterwards, the photothermal conversion efficiency of FA-CuS PENs@Fe-EGCG nanocomposites was calculated based on the method previously reported in the literature.⁶

***In vitro* stability study**

The colloidal stability and photothermal stability of the pre-synthesized nanocomposites were further investigated by DLS measurements and UV-Vis spectroscopy according to the methods published in the previous articles.^{7, 8} The hydrodynamic sizes of FA-CuS PENs@Fe-EGCG, FA-CuS PENs@EGCG, and CuS PENs@Fe-EGCG nanocomposites (0.05 mg/mL) dissolved in water, PBS,

and DMEM medium containing 10% FBS were respectively recorded at different time points (day 1, day 3, day 5, and day 7) *via* DLS measurements. Through monitoring the change trends of hydrodynamic sizes within 7 days, the colloidal stability of the nanocomposites can be evaluated. In addition, the photothermal stability of FA-CuS PENSs@Fe-EGCG nanocomposites was further assessed by recording the UV-Vis spectra of the FA-CuS PENSs@Fe-EGCG aqueous solution (0.4 mg/mL) before and after the 5 min of laser irradiation (1064 nm, 1.0 W/cm²).

***In vitro* dual-responsive release of iron ions and EGCG**

To investigate the pH and NIR laser dual-responsive release performance of FA-CuS PENSs@Fe-EGCG nanocomposites, the sustained-release devices were constructed. Specifically, FA-CuS PENSs@Fe-EGCG nanocomposites were dissolved in buffer solutions with varying pH (7.4 and 6.5) to prepare 3 mg/mL solutions. Subsequently, 1 mL of each solution was sealed into a 1000 MWCO dialysis membrane, and then placed in a 50 mL EP tube containing 19 mL of the corresponding pH buffer solution. The sustained-release devices were then subjected to shaking at 37 °C in the dark. At pre-indicated time points (0.5, 1, 2, 4, 8, 12, 24, and 48 h), the sample solution (1 mL) was collected from the outer phase buffer solution, and an equal volume of fresh pH-matched buffer solution was immediately added to maintain constant volume condition. For the laser-treated group, the dialysis membrane containing FA-CuS PENSs@Fe-EGCG solution was irradiated by NIR laser (1064 nm, 1.0 W/cm²) for 5 min before sampling at each time point. The cumulative release amounts of iron ion and EGCG in the collected sample solutions at indicated time points were finally quantified by ICP-OES and UV-Vis spectroscopy at 273 nm, respectively, following the methods reported in prior studies.^{7,9}

Evaluation of ROS generation

MB degradation assay was performed to verify the reactive oxygen species (ROS) generation ability

of FA-CuS PENS@Fe-EGCG nanocomposites with or without laser irradiation based on protocols established in the literature.^{10,11} In brief, the experiment comprised four distinct groups: MB, FA-CuS PENS@Fe-EGCG + H₂O₂ + MB, FA-CuS PENS@Fe-EGCG + H₂O₂ + MB + GSH, and FA-CuS PENS@Fe-EGCG + H₂O₂ + MB + laser. All mixtures were prepared as the groups mentioned above to ensure consistent final concentration of MB (10 µg/mL), H₂O₂ (10 mM), GSH (10 mM), and FA-CuS PENS@Fe-EGCG ([Fe] = 6 µg/mL). For the laser-treated group, the mixture was exposed to an additional laser irradiation (1064 nm, 1.0 W/cm²) for 5 min. Subsequently, the above four groups of mixtures were incubated in the dark for 6 h. Finally, the MB degradation degree of each mixture was determined by absorbance at 665 nm *via* UV-Vis spectroscopy. Simultaneously, the degradation level of MB in the prepared FA-CuS PENS@Fe-EGCG + H₂O₂ + MB solution was monitored over time (6, 12, 18, and 24 h) *via* UV-Vis absorbance at 665 nm.

The impact of pH conditions on the degradation efficiency of MB in the FA-CuS PENS@Fe-EGCG + H₂O₂ + MB solution was systematically evaluated, with specific measurements performed under pH 7.4 and pH 6.5 conditions. In brief, FA-CuS PENS@Fe-EGCG nanocomposites, H₂O₂, and MB were individually dissolved in buffer solution with pH 6.5 or 7.4, followed by thorough mixing to achieve final concentrations of 6 µg/mL Fe in FA-CuS PENS@Fe-EGCG, 10 mM H₂O₂, and 10 µg/mL MB. Subsequently, the FA-CuS PENS@Fe-EGCG + H₂O₂ + MB solution with specific pH value (6.5 or 7.4) was incubated, and the remaining MB was monitored over time *via* UV-Vis absorbance measurements at 665 nm. The degradation efficiencies of MB in the FA-CuS PENS@Fe-EGCG + H₂O₂ + MB solutions under pH 7.4 and pH 6.5 conditions were ultimately determined based on the remaining MB percentages.

To elucidate the role of EGCG in modulating the iron-catalyzed Fenton reaction, a comparative

UV-Vis spectroscopic analysis was performed. Specifically, the mixed aqueous solution containing FeCl₃ ([Fe] = 6 μg/mL), EGCG (24 μg/mL), H₂O₂ (10 mM), and MB (10 μg/mL) was prepared and incubated for 12 h. The role of EGCG was evidenced by comparing the absorbance at 665 nm in the UV-Vis spectrum of the aforementioned solution with that of the control solution consisting solely of FeCl₃, H₂O₂, and MB, with identical concentrations and incubation time.

T₁ MR relaxometry measurements

T₁ MR relaxometry of FA-CuS PENs@Fe-EGCG nanocomposites was conducted by a 0.5 T NMI20-Analyst NMR analyzing and imaging system (Shanghai Niumag Corporation, Shanghai, China). The aqueous solution of FA-CuS PENs@Fe-EGCG nanocomposites was serially diluted to prepare aqueous solutions with varying Fe concentrations (0.05-0.8 mM). These aqueous solution samples were then subjected to MR scanning, and the T₁ relaxation times were measured. The relaxivity was finally calculated by linearly fitting the inverse T₁ relaxation time (1/T₁) as a function of Fe concentration. The instrumental parameters were set based on the prior study.⁴

Cell culture

4T1 cells (a murine breast cancer cell line) and L929 cells (a mouse fibroblastic cell line) were sourced from the Institute of Biochemistry and Cell Biology, the Chinese Academy of Sciences (Shanghai, China). 4T1 cells were regularly cultured in DMEM medium containing 10% FBS, penicillin (100 U/mL) and streptomycin (100 U/mL) in a cell incubator with 5% CO₂ at 37 °C. L929 cells were cultured under analogous conditions with MEM medium instead of DMEM medium.

Specific cellular uptake assessments

4T1 cells were cultured in 12-well plates at a cell density of 2 × 10⁵ cells/well for 24 h to ensure cell adhesion. Afterwards, the medium was aspirated, and 4T1 cells were divided into two groups. One

group was treated with fresh medium supplemented with 2.5 μM FA to saturate folate receptors, while the other group received an equal volume of FA-free fresh medium. Following a 24 h incubation at 37 $^{\circ}\text{C}$, 4T1 cells with low and high folate receptor expression (referred to as 4T1-LFAR and 4T1-HFAR, respectively) were obtained.

The targeting efficiency of FA-CuS PENs@Fe-EGCG nanocomposites towards 4T1-HFAR cells was assessed using flow cytometry, confocal laser scanning microscopy (CLSM), and ICP-OES. For flow cytometric analysis, 4T1-HFAR and 4T1-LFAR cells were exposed to medium supplemented with FA-CuS PENs@Fe-EGCG nanocomposites and CuS PENs@Fe-EGCG nanocomposites, respectively, at a CuS concentration of 0.32 mM for 4 h after overnight adherence incubation. 4T1-HFAR cells incubated with an equal volume of medium containing PBS were used as the blank control. After trypsin digestion and PBS resuspension, the cell samples were subjected to flow cytometric analysis to quantify intracellular mean fluorescence and cellular uptake percentages using a FACScan analyzer (Becton Dickinson, Franklin, CA, USA). For CLSM analysis, 4T1-HFAR and 4T1-LFAR cells were seeded in 12-well plates pre-fixed with coverslips and subjected to the same incubation process as described above for flow cytometry. Subsequently, these cell samples underwent standardized steps, including PBS rinsing, fixation with glutaraldehyde (2.5%), and counterstaining with 4',6-diamidino-2-phenylindole (DAPI, 1 $\mu\text{g}/\text{mL}$). The obtained cell samples attached to the coverslips were ultimately scanned and photographed using confocal microscopy (Carl Zeiss LSM 700, Jena, Germany) with a 63 \times oil-immersion objective lens. For ICP-OES analysis, 4T1-HFAR and 4T1-LFAR cells were separately exposed to medium supplemented with FA-CuS PENs@Fe-EGCG nanocomposites at a series of Fe concentrations (0, 10, 20, 40, 80, and 100 μM) for 4 h. Subsequently, the cells underwent digestion with aqua regia, and the intracellular Fe content was determined by ICP-

OES.

Targeted MR imaging *in vitro*

4T1 cells (2×10^6 cells/well) were initially seeded in 6-well plates and cultured overnight to facilitate cell adherence. Subsequently, the cells were incubated with DMEM medium supplemented with FA-CuS PENs@Fe-EGCG nanocomposites or CuS PENs@Fe-EGCG nanocomposites at a series of Fe concentrations (0, 0.1, 0.2, 0.4, and 0.8 mM) for 4 h. Following this, the cells underwent a standardized procedure comprising PBS rinsing, trypsinization, centrifugation, and resuspension in PBS. The resulting 4T1 cell suspensions were finally subjected to MR imaging *via* a Signa HDxt 3.0 T MR imaging system (GE Healthcare, Milwaukee, WI, USA).

Cytotoxicity assay

To determine the therapeutic effect of the synthesized CuS NPs-based composites *in vitro*, CCK-8 assay was performed. Firstly, the cytotoxicity of CuS NPs-based composites towards normal mouse fibroblastic L929 cells was investigated. L929 cells (1.0×10^4 cells/well) were seeded in a 96-well plate and incubated with MEM medium overnight. Following this, the medium was replaced with fresh MEM medium supplemented with FA-CuS PENs@Fe-EGCG, CuS PENs@Fe-EGCG, or FA-CuS PENs@EGCG nanocomposites at various CuS concentrations (0-0.48 mM). Following a 24 h incubation, the cells were exposed to fresh serum-free MEM medium supplemented with 10% CCK-8 reagent and subsequently cultured for an additional 4 h. Finally, the cell viability of L929 cells was calculated according to the absorbance tested at 450 nm using a Multiskan MK3 ELISA reader (Thermo Scientific, Waltham, MA, USA).

Next, the cytotoxicity of FA-CuS PENs@Fe-EGCG, CuS PENs@Fe-EGCG, FA-CuS PENs@EGCG, FA-CuS PENs, and CuS PENs nanocomposites was assessed towards 4T1 breast

cancer cells at various CuS concentrations (0-0.48 mM) using the same methods under the identical incubation conditions as those employed for L929 cells, with the exception that DMEM medium was used instead of MEM medium. After calculating the cell viability of 4T1 cells with treatments of these nanocomposites, the half-maximal inhibitory concentrations (IC_{50}) were determined from the cell viability-dose analysis. To further evaluate the chemo/photothermal/chemodynamic synergetic therapeutic effect of FA-CuS PENSs@Fe-EGCG nanocomposites on 4T1 cells *in vitro*, CCK-8 assay was conducted. In brief, 4T1 cells (1.0×10^4 cells/well) pre-seeded in 96-well plates were exposed to DMEM medium supplemented with PBS, FA-CuS PENSs, FA-CuS PENSs@EGCG, CuS PENSs@Fe-EGCG, or FA-CuS PENSs@Fe-EGCG nanocomposites at the CuS concentration of 0.32 mM after overnight adherence post-seeding. Following 24 h of incubation, 4T1 cells with different treatments were incubated with fresh DMEM medium with or without continuous laser irradiation (1064 nm, 1.0 W/cm², 5 min). The cell viability of these cells was ultimately determined following the standard CCK-8 assay protocols. Meanwhile, statistical analysis of cell viability was conducted on the aforementioned nanocomposites-treated cells after laser irradiation for subsequent comparative analysis.

Cell apoptosis assay

An Annexin V-FITC/PI double staining assay was performed to quantify the cell apoptosis levels of 4T1 cells post-treatments with pre-synthesized nanocomposites with or without laser irradiation *via* flow cytometry. Specifically, FA-CuS PENSs@EGCG, CuS PENSs@Fe-EGCG, and FA-CuS PENSs@Fe-EGCG nanocomposites without FI modification were pre-synthesized and utilized in the cell apoptosis assay to avoid the interference from intrinsic FI fluorescence. Subsequently, 4T1 cells (2.0×10^5 cells/well) pre-seeded in 12-well plates were exposed to DMEM medium supplemented

with FA-CuS PENs@EGCG, FeCl₃, CuS PENs@Fe-EGCG, or FA-CuS PENs@Fe-EGCG nanocomposites at the CuS concentration of 0.32 mM or Fe concentration of 80 μM after overnight adherence post-seeding. Notably, the Fe concentration in the FeCl₃-containing DMEM medium ([Fe] = 80 μM) was equivalent to that in the CuS NPs-based composites-containing DMEM medium ([CuS] = 0.32 mM). Meanwhile, 4T1 cells treated with PBS were used as the blank control. Following 24 h of incubation and subsequent PBS washing, 4T1 cells treated with FA-CuS PENs@Fe-EGCG nanocomposites were subjected to laser irradiation (1064 nm, 1.0 W/cm², 5 min) or non-laser irradiation. The cell apoptosis levels of these 4T1 cells were ultimately determined following the standard Annexin V-FITC/PI apoptosis detection protocols *via* flow cytometry (FACScan analyzer, Becton Dickinson, Franklin, CA, USA).

Determination of intracellular ROS, GSH, and LPO levels *in vitro*

To explore the intracellular levels of ROS, GSH, and lipid peroxidation (LPO) in 4T1 cells following treatments with pre-synthesized nanocomposites with or without laser irradiation, DCFH-DA assay, GSH/GSSG colorimetric assay, and LPO assay were conducted using the CuS NPs-based composites without FI modification to avoid the interference from intrinsic FI fluorescence. In brief, 4T1 cells (2.0×10^5 cells/well) pre-seeded in 12-well plates were exposed to DMEM medium supplemented with materials as those used in the aforementioned cell apoptosis assay. Following 6 h of incubation and subsequent PBS washing, 4T1 cells treated with FA-CuS PENs@Fe-EGCG nanocomposites were subjected to laser irradiation (1064 nm, 1.0 W/cm², 5 min) or non-laser irradiation. The harvested 4T1 cell samples were subjected to subsequent qualitative or quantitative detection of intracellular ROS, GSH, and LPO.

For the determination of intracellular ROS, these treated cell samples were incubated for 40 min

with fresh DMEM medium supplemented with 10 μ M DCFH-DA probe in the dark and then divided into two groups. The first group of these cell samples was processed through a standardized procedure consisting of PBS rinsing, trypsinization, centrifugation, and resuspension in PBS. The resulting 4T1 cell suspensions were finally subjected to quantitative ROS detection *via* flow cytometry (FACScan analyzer, Becton Dickinson, Franklin, CA, USA). The second group of the DCFH-DA probe pretreated cell samples was sequentially processed with PBS rinsing, fixation with glutaraldehyde (2.5%), and counterstaining with DAPI for qualitative ROS detection *via* CLSM (Carl Zeiss LSM 700, Jena, Germany). For the quantification of intracellular GSH and LPO, the same rinsing, trypsinization, and resuspension steps used in the intracellular quantitative ROS detection were carried out, with the exception that GSH/GSSG colorimetric assay kit and LPO assay kit with C11-BODIPY^{581/591} probe were respectively used instead of DCFH-DA probe, following the manufacturer's protocols.

Targeted MR imaging *in vivo*

All animal experimental procedures were performed in line with the institutional guidelines approved by the Animal Ethics Committee of Nanjing Tech University (No. IACUC-20250306-70) for animal care and use. Subcutaneous xenograft tumor models were first established *via* injecting 0.1 mL of PBS containing approximately 3×10^6 4T1 cells into the right upper flank of the female BALB/c nude mice (15-20 g, 4-5 weeks old, specific pathogen-free, Shanghai SLAC Laboratory Animal Center, Shanghai, China). Once palpable tumors (0.3-0.5 cm³) formed within two weeks post-inoculation, *in vivo* experiments were initiated.

The 4T1 tumor-bearing mice pre-anesthetized with pentobarbital sodium (40 mg/kg) were divided into two groups and received intravenous injections of NS solution containing FA-CuS PENs@Fe-EGCG nanocomposites ([Fe] = 1 mM, 0.1 mL) or CuS PENs@Fe-EGCG nanocomposites

([Fe] = 1 mM, 0.1 mL). The MR imaging of these 4T1 tumor-bearing mice was performed at predetermined time points (0, 1, 2, 6, 12, and 24 h) post-administration using a Signa HDxt 3.0 T MR imaging system (GE Healthcare, Milwaukee, WI, USA) with parameters set based on established protocols from the prior study.⁴

***In vivo* thermal imaging of tumors**

For thermal imaging analysis *in vivo*, anesthetized 4T1 tumor-bearing mice were intravenously injected with FA-CuS PENs@Fe-EGCG nanocomposites ([CuS] = 4 mM, in 0.1 mL NS) or NS (0.1 mL) *via* tail vein. After 6 h, the tumor region was exposed to a 1064 nm NIR laser irradiation (1.0 W/cm²) for 5 min. Temperature variations within the tumor region and thermal images of the tumor-bearing mice were captured by a FLIR A300 thermal imaging device (IRS Systems Inc., Shanghai, China).

***In vivo* biodistribution**

The biodistribution of FA-CuS PENs@Fe-EGCG nanocomposites was assessed by quantifying Fe contents in different organs, following established protocols described in a prior study.⁴ Briefly, each tumor-bearing mouse received an intravenous injection of FA-CuS PENs@Fe-EGCG nanocomposites solution ([Fe] = 1 mM, in 0.1 mL NS). At predetermined time points (0, 3, 6, 12, 24, 48, and 72 h, respectively) post-injection, the mice were sacrificed, and their major organs along with tumors were excised for Fe quantification by ICP-OES.

***In vivo* synergetic antitumor efficacy evaluation**

Firstly, 4T1 tumor-bearing mice with comparable body weights and tumor volumes were randomly allocated into 8 groups (designated as day 0), including the FA-CuS PENs@Fe-EGCG, FA-CuS PENs@Fe-EGCG + laser, CuS PENs@Fe-EGCG + laser, FA-CuS PENs@EGCG, FA-CuS

PENs@EGCG + laser, FA-CuS PENs, FA-CuS PENs + laser, and NS. The 4T1 tumor-bearing mice were administered with the corresponding CuS NPs-based composites ([CuS] = 4 mM, in 0.1 mL NS) or NS (0.1 mL) *via* intravenous injection on day 0, 6, and 12. For the laser-treated groups, the tumor-bearing mice were exposed to laser irradiation (1064 nm, 1.0 W/cm², 5 min) at 6 h after each injection. The body weights and tumor volumes of the 4T1 tumor-bearing mice were monitored every 3 days over the 18-day administration period, with survival rates recorded daily. The relative body weight and relative tumor volume were subsequently calculated using established protocols described in a prior study.⁴ Following 18 days of administration, tumors from tumor-bearing mice in each group were excised, weighed, and photographed after euthanasia to comprehensively assess the therapeutic efficacy of a series of CuS NPs-based composites with or without laser exposure. Additionally, one mouse from each group was randomly selected for organ (heart, liver, spleen, lung, kidney) and tumor collection after euthanasia. These tissue samples were processed through standardized steps, including fixation with 10% formalin, dehydration, embedding in paraffin, and sectioning. Hematoxylin and eosin (H&E) staining was performed to assess cell necrosis in organs and tumors, while terminal deoxynucleotidyl transferase dUTP nick-end labeling (TUNEL) staining was applied to detect apoptosis levels of tumors, following established protocols described in prior studies.^{4, 7}

Blood routine and serum biochemistry assay

To confirm the biosafety of the fabricated nanocomposites, healthy nude mice were intravenously injected with FA-CuS PENs nanocomposites solution ([CuS] = 4 mM, in 0.1 mL NS), FA-CuS PENs@Fe-EGCG nanocomposites solution ([CuS] = 4 mM, in 0.1 mL NS), and NS (0.1 mL), respectively. On the 7th day post-injection, the mice were sacrificed and the blood samples were collected. First, routine blood analysis was performed using an automated blood cell counter (BC-

2800 Vet Analyzers, Mindray, Shenzhen, China) to quantify the indicators such as white blood cells (WBCs), lymphocytes (Lymph), mean corpuscular hemoglobin (MCH), mean corpuscular hemoglobin concentration (MCHC), mean corpuscular volume (MCV), granulocytes (Gran), platelets (PLTs), red blood cells (RBCs), hemoglobin (HGB), and hematocrit (HCT). Subsequently, the blood samples were subjected to centrifugation (3000-4000 rpm, 10 min) to obtain serum, and serum biochemistry indicators, including liver function markers (alanine aminotransferase (ALT) and aspartate aminotransferase (AST)), and kidney function markers (creatinine (CREA), uric acid (UA), and urea (UREA)) were analyzed by Servicebio Technology Co., Ltd. (Wuhan, China).

Statistical analysis

All data were expressed as the mean \pm standard deviation ($n \geq 3$). Statistical significance was determined by a one-way ANOVA statistical method, with significance levels denoted as follows: (*) for $p < 0.05$, (**) for $p < 0.01$, and (***) for $p < 0.001$, respectively.

Table S1. Quantification of Cu and Fe loaded within different nanocomposites.

Sample	Weight percentage	Weight percentage	Loading number
	of Cu (wt%)	of Fe (wt%)	of Fe
FA-CuS PENs@Fe-EGCG	3.04%	0.67%	8.3
FA-CuS PENs@EGCG	3.06%	/	/
CuS PENs@Fe-EGCG	3.33%	0.73%	9.1

Table S2. Drug loading amount (DL), encapsulation efficiency (EE) and loading number of EGCG in different nanocomposites.

Sample	DL (wt%)	EE (wt%)	Loading number of EGCG
FA-CuS PENs@Fe-EGCG	12.1%	96.0%	18.7
FA-CuS PENs@EGCG	12.0%	92.8%	18.1
CuS PENs@Fe-EGCG	12.9%	95.1%	18.5

Table S3. Zeta potentials, hydrodynamic sizes and polydispersity indexes (PDI) of FA-CuS PENs, FA-CuS PENs@EGCG and FA-CuS PENs@Fe-EGCG nanocomposites dissolved in water at room temperature.

Sample	Zeta potential (mV)	Hydrodynamic size (nm)	PDI
FA-CuS PENs	8.4 ± 0.4	70.7 ± 6.2	0.34 ± 0.07
FA-CuS PENs@EGCG	-0.7 ± 0.1	104.6 ± 3.2	0.42 ± 0.01
FA-CuS PENs@Fe-EGCG	-1.5 ± 0.2	99.6 ± 2.4	0.29 ± 0.01

Table S4. IC₅₀ values of FA-CuS PENs@Fe-EGCG, FA-CuS PENs@EGCG, and CuS PENs@Fe-EGCG nanocomposites on 4T1 cells.

Sample	FA-CuS PENs@ Fe-EGCG	FA-CuS PENs@ EGCG	CuS PENs@ Fe-EGCG
IC ₅₀ ([Cu] mM)	0.33	0.43	0.36

Table S5. Flow cytometric assay performed using Annexin V-FITC/PI double staining of 4T1 cells after different treatments. The percentages of necrotic (Q1), late apoptotic (Q2), early apoptotic (Q3), and viable (Q4) cells were recorded, respectively.

Treatment	Necrotic cells (%)	Late apoptotic cells (%)	Early apoptotic cells (%)	Viable cells (%)
PBS	4.23 ± 0.59	3.75 ± 0.42	1.21 ± 0.06	90.79 ± 0.48
FA-CuS PENs@EGCG	7.90 ± 0.82	5.34 ± 0.19	2.24 ± 0.16	84.52 ± 0.63
FeCl ₃	4.47 ± 0.48	9.37 ± 0.17	1.66 ± 0.13	84.48 ± 0.39
CuS PENs@Fe-EGCG	5.27 ± 0.57	17.0 ± 0.30	3.75 ± 0.03	73.96 ± 0.74
FA-CuS PENs@Fe-EGCG	3.0 ± 0.23	23.77 ± 0.61	11.30 ± 0.10	61.94 ± 0.42
FA-CuS PENs@Fe-EGCG + laser	2.34 ± 0.16	43.40 ± 0.70	4.63 ± 0.38	49.67 ± 0.35

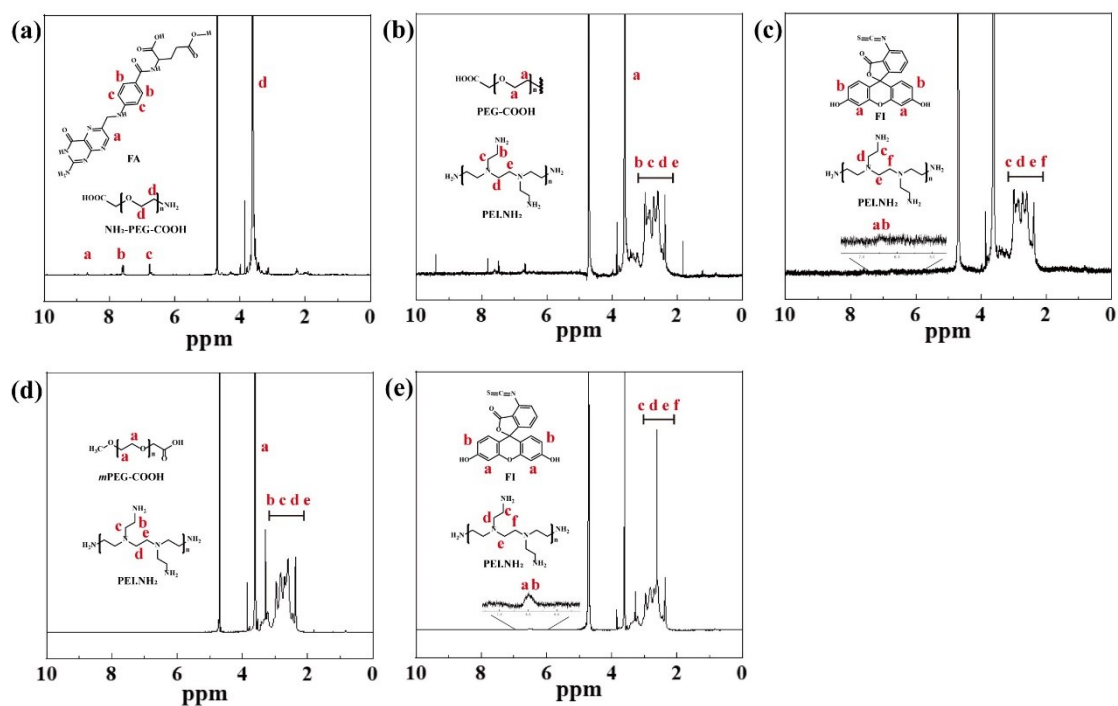


Fig. S1 ^1H NMR spectra of (a) FA-PEG-COOH, (b) PEI.NH₂-(PEG-FA), (c) PEI.NH₂-(PEG-FA)-FI, (d) PEI.NH₂-*m*PEG, and (e) PEI.NH₂-*m*PEG-FI dispersed in D₂O, respectively.

The presence of the characteristic peaks of FA (6.7 ppm, 7.6 ppm, and 8.7 ppm) and NH₂-PEG-COOH (3.4-3.8 ppm) in the ^1H NMR spectrum of FA-PEG-COOH indicates the successful modification of FA onto NH₂-PEG-COOH (Fig. S1a). Following the conjugation of FA-PEG-COOH and FI to the surface of PEI.NH₂, the characteristic peaks of FA-PEG-COOH (3.4-3.8 ppm), FI (6.4 ppm), and PEI.NH₂ (2.3-3.1 ppm) appeared in the ^1H NMR spectra of PEI.NH₂-(PEG-FA) and PEI.NH₂-(PEG-FA)-FI, respectively, indicating the successful conjugation of FA-PEG-COOH and FI moieties to PEI.NH₂. These results manifest the successful formation of PEI.NH₂-(PEG-FA) and PEI.NH₂-(PEG-FA)-FI (Fig. S1b and c). Furthermore, the degree of conjugation was quantified by integrating the characteristic peaks of FA, PEG, FI, and PEI.NH₂ in these ^1H NMR spectra. It can be determined that approximately 13.9 FA-PEG-COOH, 9.7 FA, and 2.6 FI moieties are linked to each PEI.NH₂, as calculated using a previously published method.¹ Similarly, the same analytical and quantitative methods were applied to the FA-free nanosystem PEI.NH₂-*m*PEG-FI. Quantitative

analysis of the characteristic peaks of *m*PEG-COOH (3.4-3.8 ppm) and FI (6.4 ppm) in the ¹H NMR spectra of PEI.NH₂-*m*PEG and PEI.NH₂-*m*PEG-FI reveals that the comparable functional moieties (13.3 *m*PEG-COOH and 2.3 FI) are linked to PEI.NH₂-*m*PEG-FI (Fig. S1d and e).

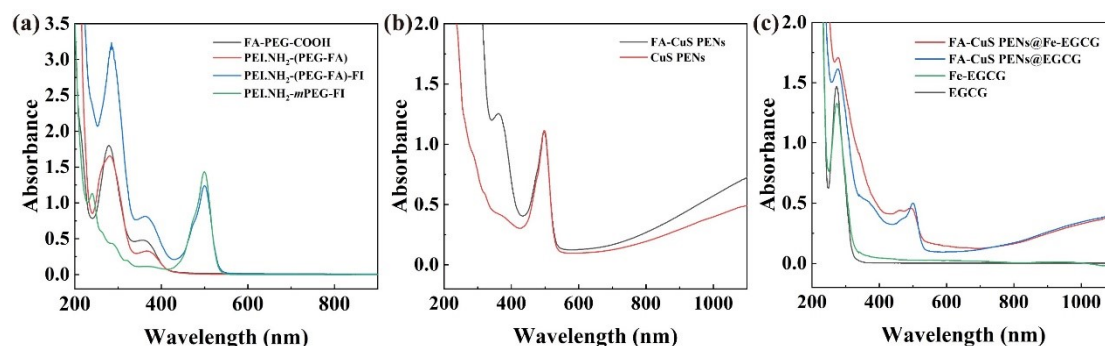


Fig. S2 UV-Vis spectra of (a) FA-PEG-COOH, PEI.NH₂-(PEG-FA), PEI.NH₂-(PEG-FA)-FI, PEI.NH₂-*m*PEG-FI, (b) FA-CuS PENS, CuS PENS and (c) FA-CuS PENS@Fe-EGCG, FA-CuS PENS@EGCG, Fe-EGCG, and EGCG dispersed in water, respectively.

As shown in Fig. S2a, the UV-Vis spectrum of PEI.NH₂-(PEG-FA)-FI simultaneously displays distinct absorption peaks of FA (279 and 357 nm) and FI (500 nm), suggesting the successful conjugation of FA and FI to the polyethylenimine derivative. Similarly, the UV-Vis spectrum of the FA-free nanosystem PEI.NH₂-*m*PEG-FI displays the characteristic absorption peak of FI at 500 nm, demonstrating the successful FI conjugation to PEI.NH₂-*m*PEG. Furthermore, FA-CuS PENS and CuS PENS nanocomposites (synthesized *via in situ* growth of CuS NPs within the internal cavity of polyethylenimine derivatives) exhibit the broad UV-Vis absorption peak of CuS NPs (1000-1100 nm) in the NIR window II. This NIR absorption peak is attributed to the d-d energy band transition of copper ions, indicating the successful formation of CuS NPs (Fig. S2b), in accordance with the prior study.² Finally, the UV-Vis spectra of Fe-EGCG, FA-CuS PENS@Fe-EGCG nanocomposites, and FA-CuS PENS@EGCG nanocomposites all exhibit an absorption peak at 273 nm, which is consistent

with that of EGCG, thereby validating the successful loading of EGCG onto FA-CuS PENs nanocomposites (Fig. S2c).

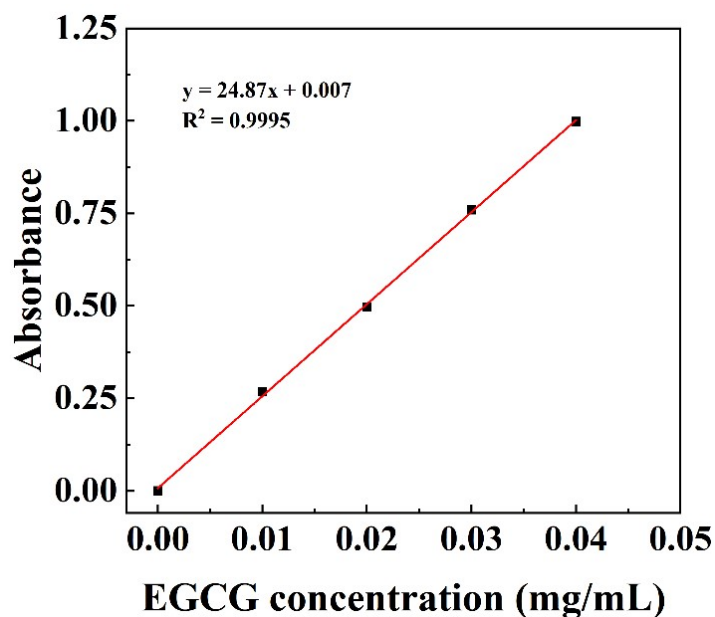


Fig. S3 Standard curve of EGCG dispersed in water determined by UV-Vis absorbance at 273 nm.

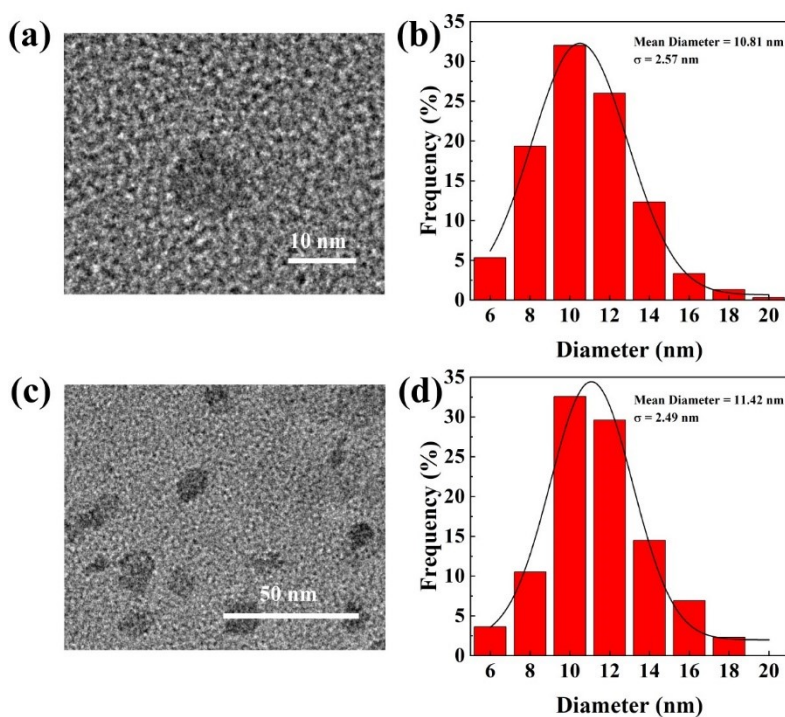


Fig. S4 (a) High-resolution TEM image and (b) size distribution histogram of FA-CuS PENs@Fe-EGCG nanocomposites. (c) TEM image and (d) size distribution histogram of FA-CuS PENs@EGCG nanocomposites.

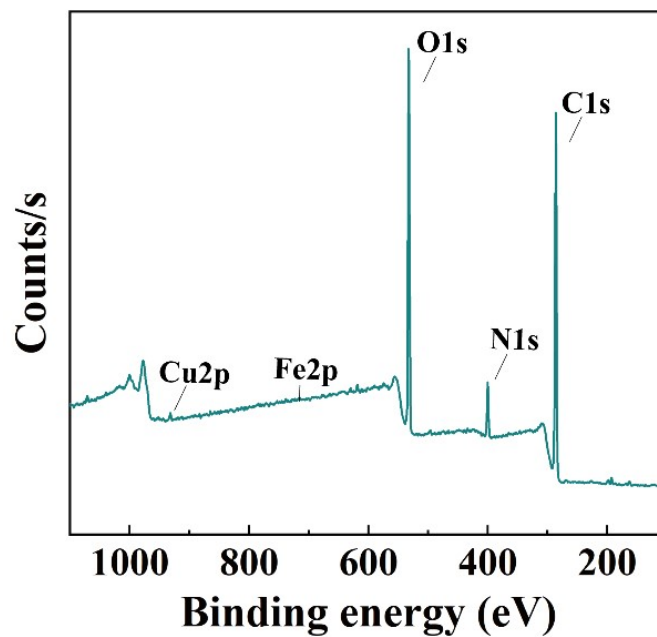


Fig. S5 XPS spectrum of FA-CuS PENs@Fe-EGCG nanocomposites.

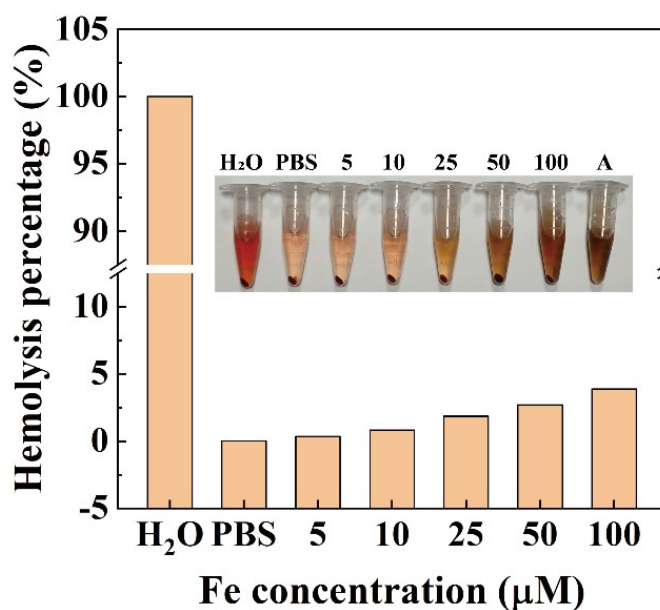


Fig. S6 The hemolysis rate and the corresponding photograph of red blood cells treated with different Fe concentrations of FA-CuS PENs@Fe-EGCG nanocomposites for 2 h, in which sample A is FA-CuS PENs@Fe-EGCG nanocomposites solution ($[Fe] = 100 \mu M$) without red blood cells.

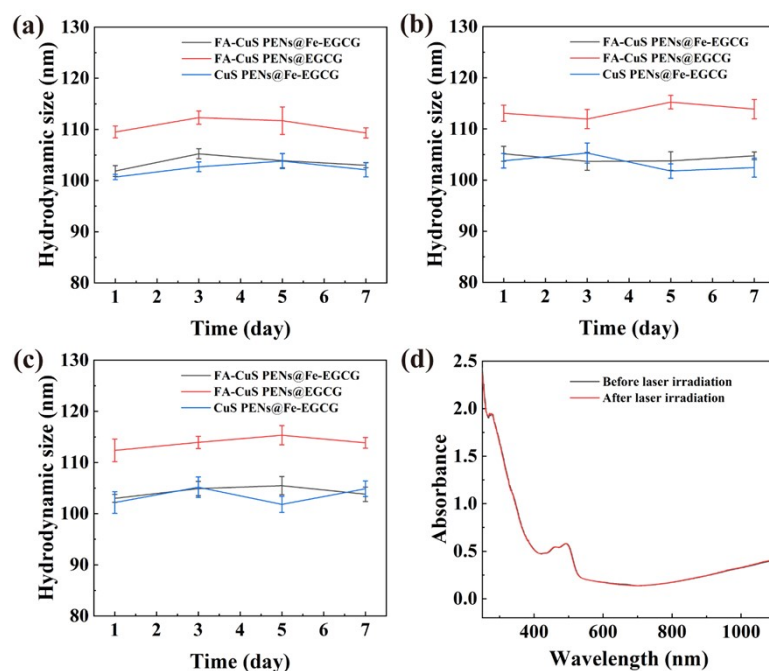


Fig. S7 Hydrodynamic size curves of FA-CuS PENs@Fe-EGCG, FA-CuS PENs@EGCG, and CuS PENs@Fe-EGCG nanocomposites dissolved in (a) water, (b) PBS, and (c) DMEM medium containing 10% FBS over time. (d) UV-Vis spectra of FA-CuS PENs@Fe-EGCG aqueous solution before and after 1064 nm laser irradiation (1.0 W/cm², 5 min).

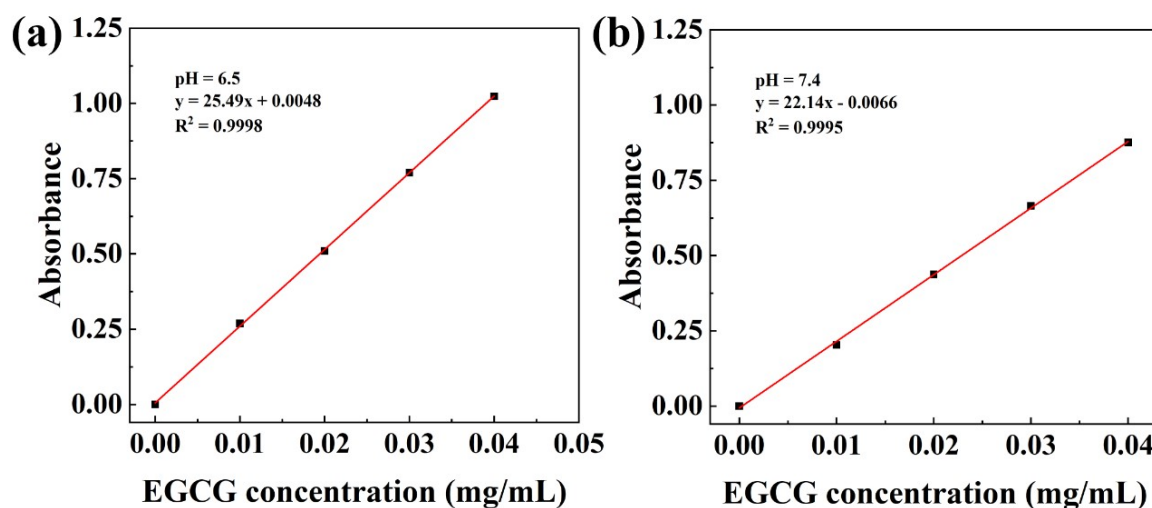


Fig. S8 Standard curves of EGCG dispersed in (a) pH 6.5 buffer solution and (b) pH 7.4 buffer solution determined by UV-Vis absorbance at 273 nm.

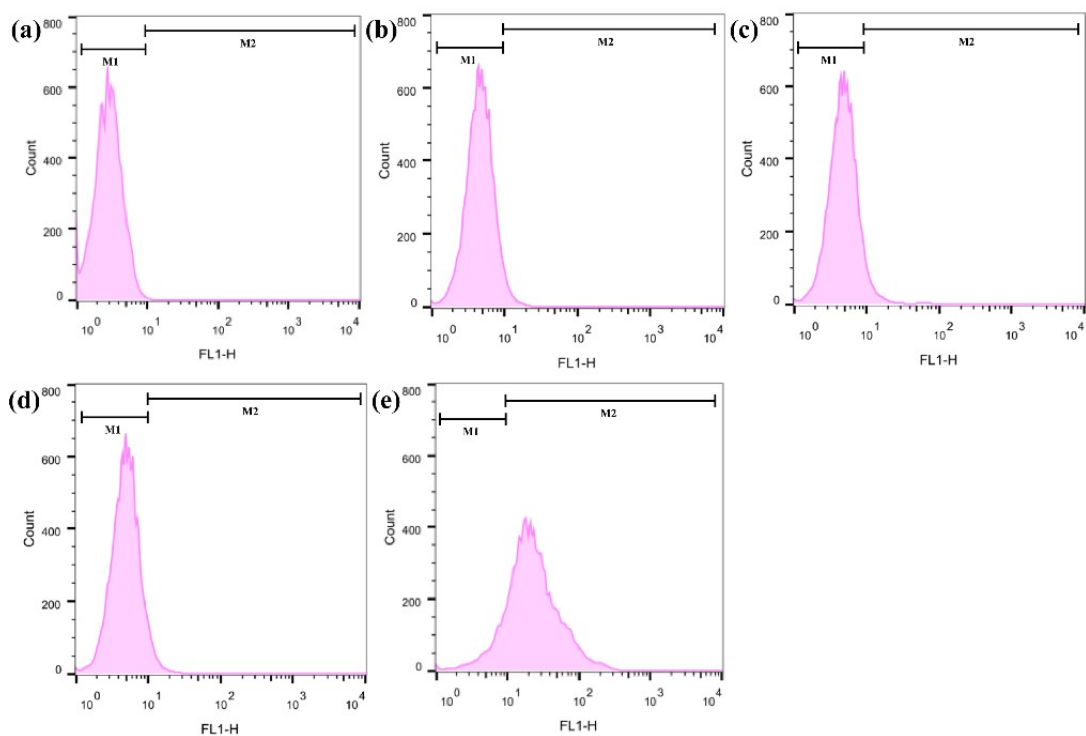


Fig. S9 Flow cytometric analysis of (a) 4T1-HFAR cells treated with PBS, (b) 4T1-LFAR and (c) 4T1-HFAR cells treated with CuS PENs@Fe-EGCG nanocomposites, (d) 4T1-LFAR and (e) 4T1-HFAR cells treated with FA-CuS PENs@Fe-EGCG nanocomposites for 4 h, respectively.

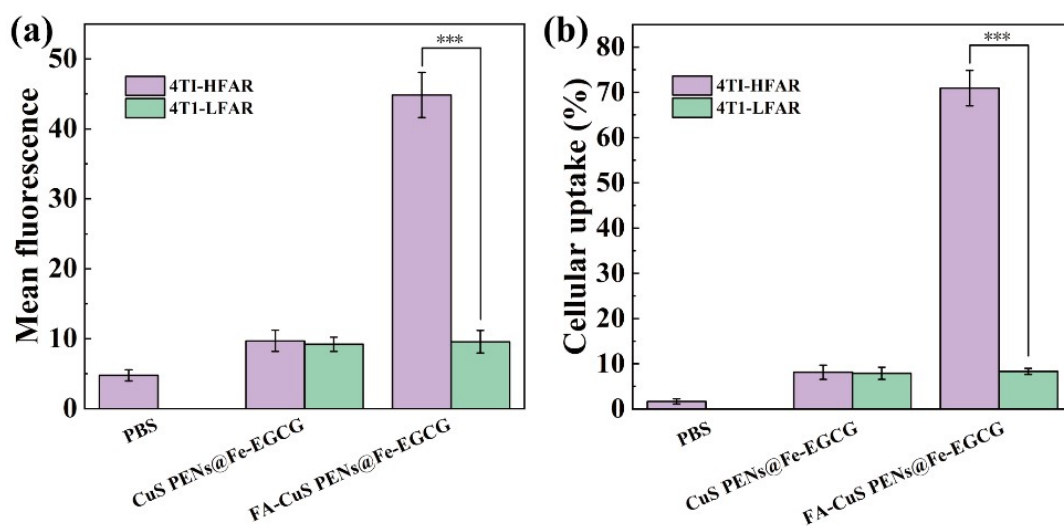


Fig. S10 Flow cytometric quantification of (a) intracellular mean fluorescence and (b) cellular uptake percentages of 4T1-HFAR and 4T1-LFAR cells after 4 h treatment with different nanocomposites, respectively.

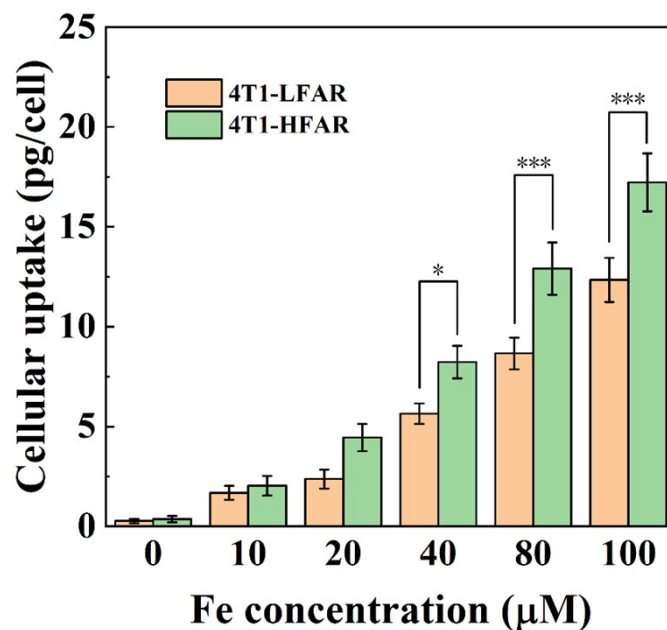


Fig. S11 Cellular uptake of Fe in 4T1-LFAR and 4T1-HFAR cells assessed by ICP-OES after 4 h co-incubation with FA-CuS PENs@Fe-EGCG nanocomposites at different Fe concentrations, respectively.

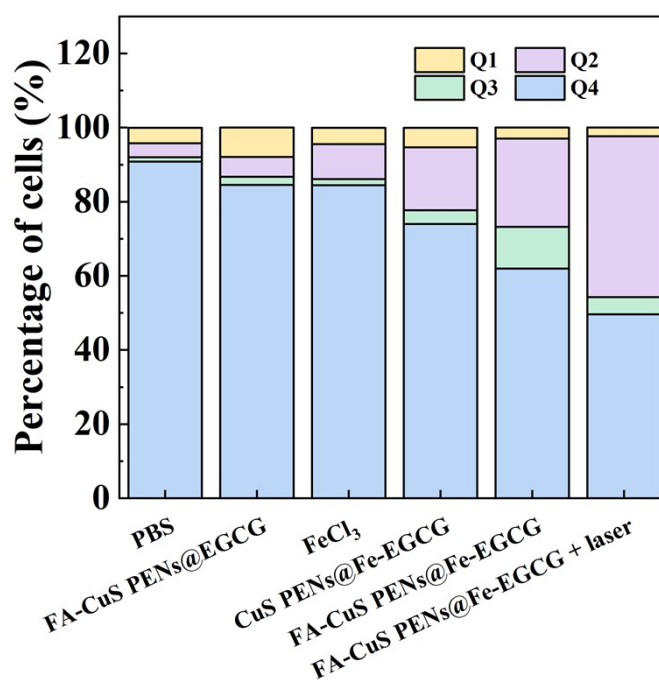


Fig. S12 Flow cytometric analysis of 4T1 cells after different treatments using Annexin V-FITC/PI double staining, revealing the percentage distribution of necrotic (Q1), late apoptotic (Q2), early apoptotic (Q3), and viable (Q4) cells.

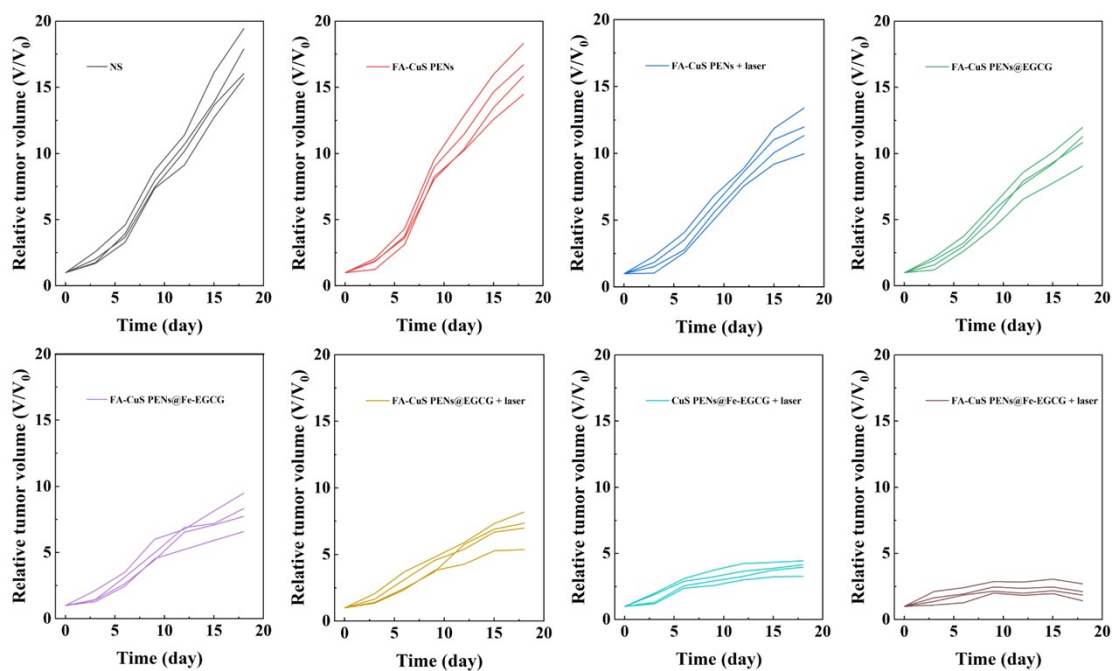


Fig. S13 Individual tumor growth curves of 4T1 tumor-bearing mice after different treatments.

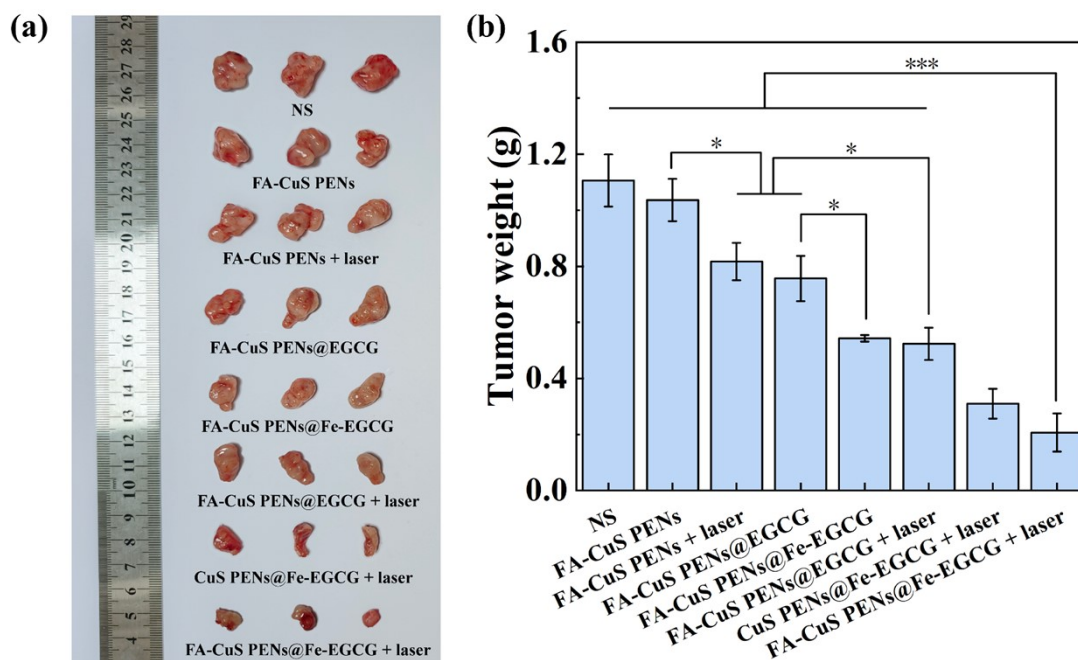


Fig. S14 (a) Representative photographs of excised tumors and (b) the corresponding tumor weights of 4T1 tumor-bearing mice after different treatments.

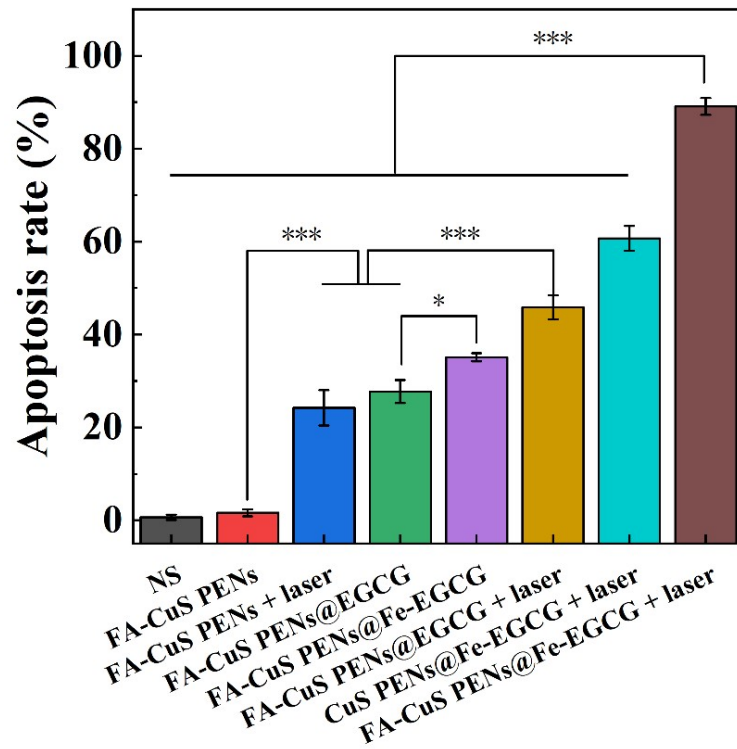


Fig. S15 The apoptosis rate of tumor tissues with different treatments recorded from TUNEL stained sections.

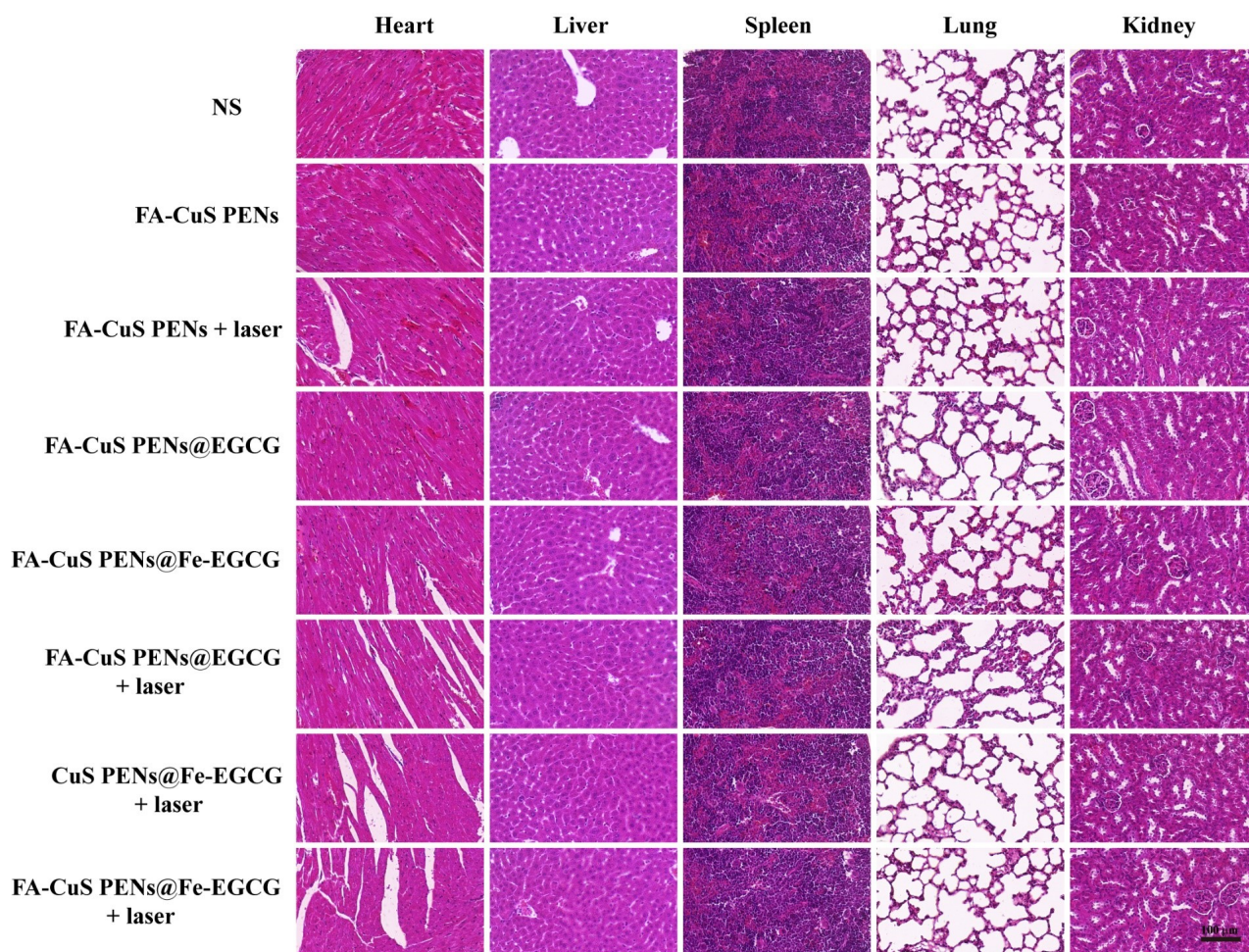


Fig. S16 H&E staining of major organs from 4T1 tumor-bearing mice after different treatments. The scale bar represents 100 μm .

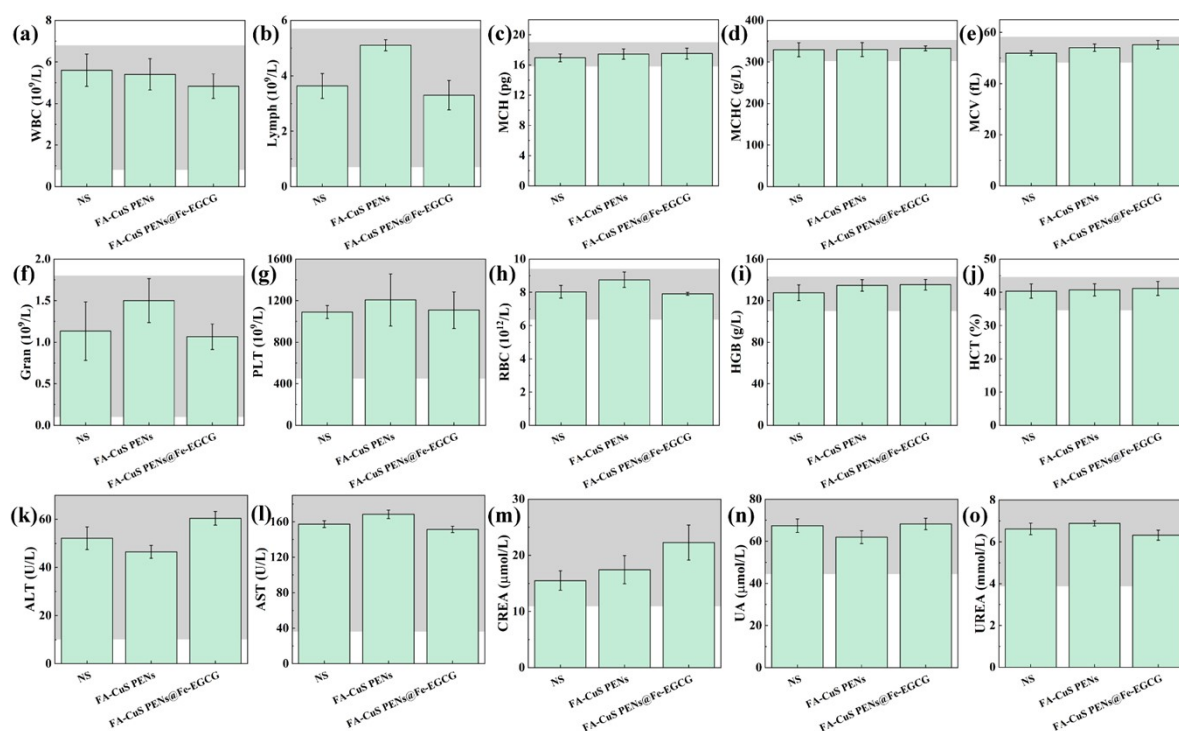


Fig. S17 Blood routine analysis and serum biochemistry analysis of nude mice on the 7th day post-injection of NS, FA-CuS PENs, or FA-CuS PENs@Fe-EGCG nanocomposites. Blood routine analysis included (a) WBCs, (b) Lymph, (c) MCH, (d) MCHC, (e) MCV, (f) Gran, (g) PLTs, (h) RBCs, (i) HGB, and (j) HCT. Serum biochemistry analysis included (k) ALT, (l) AST, (m) CREA, (n) UA, and (o) UREA. The shaded area denotes the normal range of each indicator.

References

1. J. Y. Zhu, L. F. Zheng, S. H. Wen, Y. Q. Tang, M. W. Shen, G. X. Zhang and X. Y. Shi, *Biomaterials*, 2014, **35**, 7635-7646.
2. Y. M. Zhang, Z. J. Ouyang, M. S. Zhan, R. Yang, Y. Gao, L. L. Li, R. Guo, X. Y. Shi and X. Y. Cao, *Small*, 2023, **19**, 202301914.
3. M. Wang, A. Yu, W. Han, J. Chen, C. Lu and X. Tu, *Mater. Today Bio*, 2024, **26**, 101040.
4. Z. Q. Wang, Y. Q. Guo, Y. Fan, J. W. Chen, H. Wang, M. W. Shen and X. Y. Shi, *Adv. Mater.*,

2021, **34**, 2107009.

5. Y. C. Hao, Y. Gao, Y. Fan, C. C. Zhang, M. S. Zhan, X. Y. Cao, X. Y. Shi and R. Guo, *J. Nanobiotechnol.*, 2022, **20**, 43.
6. Z. J. Ouyang, D. Li, Z. J. Xiong, C. Song, Y. Gao, R. N. Liu, M. W. Shen and X. Y. Shi, *ACS Appl. Mater. Interfaces*, 2021, **13**, 6069-6080.
7. L. Y. Zhang, G. M. Li, Z. J. Ouyang, R. Yang, Y. Gao, X. Y. Cao, I. Bányai, X. Y. Shi and R. Guo, *Biomater. Sci.*, 2022, **10**, 2029-2039.
8. H. Z. Yu, M. Ma, K. C. Liang, J. Shen, Z. Y. Lan and H. R. Chen, *Appl. Mater. Today*, 2021, **25**, 101235.
9. X. Y. Meng, J. Y. Wu, Z. F. Hu and X. W. Zheng, *J. Mater. Chem. B*, 2024, **12**, 1285-1295.
10. M. Mu, H. F. Chen, R. R. Fan, Y. L. Wang, X. Tang, L. Mei, N. Zhao, B. W. Zou, A. P. Tong, J. G. Xu, B. Han and G. Guo, *J. Adv. Res.*, 2021, **34**, 29-41.
11. M. Q. Huang, E. H. Wang, X. J. Li, Z. Y. Wei, T. T. Wang, A. Wang and L. Yang, *ACS Appl. Nano Mater.*, 2024, **7**, 10928-10940.